Field dependence of the hyperfine splitting of holmium in holmium hydroxide

1989 J. Phys.: Condens. Matter 1 1309

(http://iopscience.iop.org/0953-8984/1/7/014)

J. Phys.: Condens. Matter 1 (1989) 1309–1327. Printed in the UK

Field dependence of the hyperfine splitting of holmium in holmium hydroxide

D St P Bunbury, C Carboni and M A H McCausland
The Schuster Laboratory, The University, Manchester M13 9PL, UK

Received 25 July 1988

Abstract. The hyperfine splitting of ^{165}Ho in holmium hydroxide has been studied by spin-echo NMR at liquid-helium temperatures in fields up to 8 T. The behaviour of the dipolar splitting in fields below 0.5 T confirms that the hyperfine parameters are not thermally averaged and that the NMR signals arise solely from ions in the electronic ground state. The field dependence of the hyperfine splitting is not accurately described by crystal-field parameters derived from magnetic susceptibility measurements on $Ho(OH)_3$, but is in close agreement with calculations based on parameters derived from optical spectroscopy of Ho^{3+} in $Y(OH)_3$. The following quantities are derived from our measurements: spontaneous magnetisation and longitudinal susceptibility of $Ho(OH)_3$ at $T = 0$: $M_0 = (1.181 \pm 0.001)$ MA m^{-1} and $\chi_\parallel = 0.0146 \pm 0.0005$; ratio of nuclear to electronic anti-shielding factors for Ho^{3+} in the hydroxide: $\gamma_N/\gamma_E = 149 \pm 15$.

1. Introduction

The rare-earth hydroxides, $R(OH)_3$, are singularly well adapted for quantitative studies of uniaxial crystal-field anisotropy. Their hexagonal structure (space group C^2_{6h}) is combined with a needle-like crystal habit that facilitates magnetic measurements (Christensen *et al* 1967, Mroczkowski *et al* 1970). The two lanthanide sites in the unit cell are equivalent and have C_{3h} point symmetry. The interaction of the lanthanide (R^{3+}) ions with the crystalline electric field is therefore described by four crystal-field parameters.

Detailed information about crystal-field splittings of several R^{3+} ions in the pure hydroxides and in the isostructural $Y(OH)_3$ compounds has been obtained from high-resolution optical spectroscopy (Scott *et al* 1969, Scott 1970, Cone 1972, Kahle *et al* 1986; see also the review article of Morrison and Leavitt 1982). The crystal-field parameters thus obtained provide a quantitative basis for theoretical interpretation of the magnetic properties of the hydroxides. Conversely, static and dynamic magnetisation measurements provide useful tests of the parameters derived from optical spectroscopy. The hydroxides have in fact been extensively studied by magnetisation, susceptibility, and paramagnetic resonance measurements (Wolf *et al* 1968, Scott *et al* 1969, Scott 1970, Schlachetzki and Eckert 1972, Skjeltorp *et al* 1973, Catanese and Meissner 1973, Catanese *et al* 1973). Measurements of hyperfine splittings can provide particularly delicate tests of theoretical models but the only such measurements so far reported on the hydroxides are a zero-field Mössbauer study of antiferromagnetic $Gd(OH)_3$ (Katila *et al* 1972), a zero-field NMR study of ferromagnetic $Ho(OH)_3$ (Bunbury *et al* 1985, to be referred to as I) and a brief report of the field dependence of the hyperfine splitting of

0953-8984/89/071309 + 19 $02.50

Table 1. Lattice parameters of the hydroxides of holmium, yttrium and erbium; magnetic properties of $Ho(OH)_3$.

	Lattice parameters[a] (nm)			Magnetic properties[b]			
	a	b	c/a	T_c (K)	M_{sat} (MA m^{-1})	$\chi_{\parallel}$	χ_{-}
$Ho(OH)_3$	0.6255	0.3545	0.5667	2.54	1.14 ± 0.02	<0.025	0.13 ± 0.04
$Y(OH)_3$	0.6241	0.3539	0.5671				
$Er(OH)_3$	0.6232	0.3518	0.5645				

[a] Christensen *et al* (1967).

[b] After Catanese and Meissner (1973). The saturation magnetisation and susceptibilities, measured at 1.1 K, have been converted into SI units.

holmium in $Y(OH)_3$ (Bunbury *et al* 1986).

The lanthanide ions in the hydroxides are closely spaced along the c direction; the spacing in the basal plane is much larger (see table 1). Thus the ions belonging to alternate hexagonal planes form chains of practically contiguous neighbours: to a first approximation, we may picture the lanthanide sub-lattice in terms of one-dimensional arrays of weakly interacting but strongly anisotropic moments. The nature of the interaction between the lanthanide ions has been discussed by Wolf *et al* (1968), Cochrane *et al* (1971), Skjeltorp *et al* (1973), Catanese *et al* (1973), Catanese and Meissner (1973), Cone and Wolf (1978) and Kahle *et al* (1986). The interaction is predominantly dipolar, but there is a significant exchange term and a small electric multipolar contribution. Spontaneous magnetic order, where it occurs at all, does so only at temperatures below 4 K. Crystal-field splittings for non-S-state ions in the hydroxides are of the order of 500 K, so the inter-ionic interaction is much weaker than the crystal-field interaction.

The sign of the crystal-field anisotropy in the hydroxides of terbium, dysprosium and holmium is such that the c axis is the preferred direction of magnetisation. Tb^{3+} and Ho^{3+}, though non-Kramers ions, have crystal-field ground states that are magnetic doublets and so behave in a similar manner to the Kramers ion Dy^{3+}. All three compounds have strongly uniaxial properties at low temperatures, and exhibit Ising-like ferromagnetic order in the liquid-helium range (Wolf *et al* 1968, Catanese and Meissner 1973, Catanese *et al* 1973).

In I we showed that zero-field hyperfine splitting of ^{165}Ho in the ferromagnetic phase of holmium hydroxide agrees well with calculations based on optically derived crystal-field parameters. The field dependence of the hyperfine splitting, to be described in the present paper, provides a more thorough test of the theory and, as we shall see, confirms that the hyperfine splitting is not thermally averaged.

2. Theory

2.1. Introduction

As noted by Cone and Faulhaber (1971), the electronic energy levels in a crystalline compound ought strictly to be regarded as excitons. Cone (1972), however, has shown that the single-ion picture adequately describes the electronic energy levels of Er^{3+} in $Er(OH)_3$ and we have no reason to suppose that the same is not true of $Ho(OH)_3$. Our calculation of the hyperfine parameters is therefore based on the conventional single-ion model in which mutual interactions are approximated by a molecular field. (See, for

example, McCausland and Mackenzie 1979 or Prakash *et al* 1984.)

The theory of the ionic energy levels and of their hyperfine splitting is the same as that outlined in I except for the addition of the applied field. The field affects the hyperfine splitting directly, by interacting with the nuclear dipole moment, and indirectly, by perturbing the electronic ground state of the parent ion. The second mechanism, as we shall see, is the more important; moreover, it affects the quadrupolar as well as the dipolar splitting. As our measurements were made at low temperatures, we are directly concerned only with the nominally $^5I_8$ ground multiplet of the ion. (The next multiplet, $^5I_7$, is over 7000 K higher.) It should be noted, however, that the ground multiplet of the free Ho^{3+} ion contains a significant admixture of $^3K_8$ states (Wybourne 1962); the effects of intermediate coupling cannot, therefore, be ignored. A further complication, namely J-mixing, can in principle arise when the ion is embedded in a solid. Unlike intermediate coupling, which, in the present context, can be dealt with by appropriate corrections to the Landé g-factor and to the operator-equivalent coefficients for the ground multiplet, J-mixing entails a major extension of the formalism. This does not seem justified in the present work because, as shown by Scott (1970), J-mixing is a rather small effect in $Ho(OH)_3$; its influence on the hyperfine interaction is unlikely to exceed uncertainties arising from other sources.

2.2. *The electronic Hamiltonian*

As in I the nominally $^5I_8$ ground multiplet of the Ho^{3+} ion is described by the Hamiltonian

$$\mathcal{H}_{el} = \mathcal{H}_{cf} + \mathcal{H}_z \tag{1}$$

where

$$\mathcal{H}_{cf} = B_2^0 O_2^0 + B_4^0 O_4^0 + B_6^0 O_6^0 + B_6^6 O_6^6 \tag{2}$$

is the crystal field interaction in the notation of Abragam and Bleaney (1971) and

$$\mathcal{H}_z = -\boldsymbol{B} \cdot \boldsymbol{\mu} \tag{3}$$

is the Zeeman interaction of the ionic moment $\boldsymbol{\mu} = -g\mu_B \boldsymbol{J}$ with the total field

$$\boldsymbol{B} = \boldsymbol{B}_a + \boldsymbol{B}_m \tag{4}$$

seen by the ion. Here $\boldsymbol{B}_a$ is the applied field; $\boldsymbol{B}_m$ is the molecular field which subsumes, in the mean-field approximation, the dipolar and exchange interactions of the ion with its neighbours (see § 2.3).

Except for some ancillary experiments, the measurements to be described were carried out with $\boldsymbol{B}_a$ collinear with the crystallographic $\boldsymbol{c}$ axis. Then $\boldsymbol{B}_m$, hence $\boldsymbol{B}$, are also collinear with the $\boldsymbol{c}$ axis. It will be convenient to define the positive $\boldsymbol{c}$ direction to be *anti*parallel to the applied field. Equation (3) then takes the form

$$\mathcal{H}_z = -g\mu_B B J_c \tag{5}$$

where $B = B_a + B_m$ is the algebraic sum of the $-\boldsymbol{c}$ components of $\boldsymbol{B}_a$ and $\boldsymbol{B}_m$. The sign convention used here ensures that $\langle J_c \rangle$, and hence the magnetic dipole hyperfine parameter, is positive in the electronic ground state.

2.2.1. The crystal-field parameters. The coefficients B_n^m in equation (2) should not be confused with the crystal-field parameters 'B_n^m' quoted by Scott (1970) and by Karmarkar *et al* (1981a, b), here denoted by $\langle r^n \rangle A_n^m$ as in Abragam and Bleaney (1971). The two

Table 2. Operator-equivalent coefficients for Ho^{3+}; crystal-field parameters (in K) for Ho^{3+} in $Y(OH)_3$ and in $Ho(OH)_3$.

		Ho : $Y(OH)_3$[b]		$Ho(OH)_3$[c]	
n, m	$\langle J\|\alpha_n\|J\rangle$[a]	$\langle r^n\rangle A_n^m$ (K)	B_n^m (K)	$\langle r^n\rangle A_n^m$ (K)	B_n^m (K)
2, 0	-2.040×10^{-3}	354 ± 5	-0.722 ± 0.010	288 ± 3	-0.588 ± 0.006
4, 0	-3.082×10^{-5}	-81.5 ± 2.0	$(2.51 \pm 0.06) \times 10^{-3}$	-82.0 ± 0.7	$(2.53 \pm 0.02) \times 10^{-3}$
6, 0	-1.203×10^{-6}	-57.3 ± 0.4	$(6.89 \pm 0.05) \times 10^{-5}$	-57.5 ± 0.7	$(6.92 \pm 0.08) \times 10^{-5}$
6, 6	-1.203×10^{-6}	782 ± 5	$(-9.41 \pm 0.06) \times 10^{-4}$	576 ± 7	$(-6.93 \pm 0.09) \times 10^{-4}$

[a] Rajnak and Krupke (1967).
[b] Scott (1970).
[c] Karmakar *et al* (1981a, b).

sets of parameters are related by

$$B_n^m = \langle J\|\alpha_n\|J\rangle\langle r^n\rangle A_n^m \tag{6}$$

where the $\langle J\|\alpha_n\|J\rangle$ are operator-equivalent coefficients†. For future reference we note that the second-order (quadrupolar) crystal-field parameter B_2^0 is related to V_{cc}, the axial component of the extra-ionic electric field gradient, by

$$B_2^0 = -(e/4)\langle J\|\alpha_2\|J\rangle\langle r^2\rangle\gamma_E V_{cc} \tag{7}$$

where γ_E is the electronic antishielding factor in the notation of Edmonds (1963). ($\gamma_E = 1 - \sigma_2$ in the notation of Blok and Shirley (1966).)

As in I, we use the operator-equivalent coefficients given by Rajnak and Krupke (1967) for the ground multiplet of Ho^{3+} with intermediate coupling. The coefficients are listed in table 2, together with the crystal-field parameters derived by Scott (1970) from the optical spectrum of Ho^{3+} in $Y(OH)_3$ at 77 K and those obtained by Karmakar *et al* (1981a, b) from magnetic susceptibility measurements on pure $Ho(OH)_3$ in the range 80–300 K. All other ionic and nuclear parameters used in our calculations will be found in Appendix 2.

It will be noted that the values of $\langle r^2\rangle A_2^0$ and $\langle r^6\rangle A_6^6$ given by Karmarkar and co-workers for the pure compound are 20–25% smaller than those given by Scott for the dilute material. On the other hand, Scott's crystal-field parameters for Ho^{3+} : $Y(OH)_3$ agree well with his relatively limited optical data on pure $Ho(OH)_3$; they also give a satisfactory account of the magnetisation, low-temperature heat capacity and zero-field hyperfine splitting of the pure compound (Catanese and Meissner 1973, Chirico *et al* 1981, I). There is therefore considerable evidence to suggest that the crystal-field parameters for Ho^{3+} are not appreciably affected by dilution with yttrium, at least at low temperatures. This accords with the work of Cone (1972), who finds no significant difference between the crystal-field parameters for Er^{3+} in $Er(OH)_3$ and in $Y(OH)_3$. $Ho(OH)_3$, like $Er(OH)_3$, has lattice parameters close to those of $Y(OH)_3$ (see table 1).

2.2.2. Electronic energy levels, eigenstates and expectation values. The energy levels and eigenstates of the ground multiplet of the Ho^{3+} ion have been computed by diagonalising $\mathcal{H}_{el}$ (equation (1)) for various values of the total field B. The field dependence of the three lowest energy levels, calculated from Scott's crystal-field parameters, is shown in figure 1; in table 3 we express the corresponding eigenstates $|E_0\rangle$, $|E_1\rangle$ and $|E_2\rangle$ at $B_a =$

† $\langle J\|\alpha_2\|J\rangle$, $\langle J\|\alpha_4\|J\rangle$ and $\langle J\|\alpha_6\|J\rangle$ correspond, respectively, to α, β and γ in Rajnak and Krupke (1967) and in I.

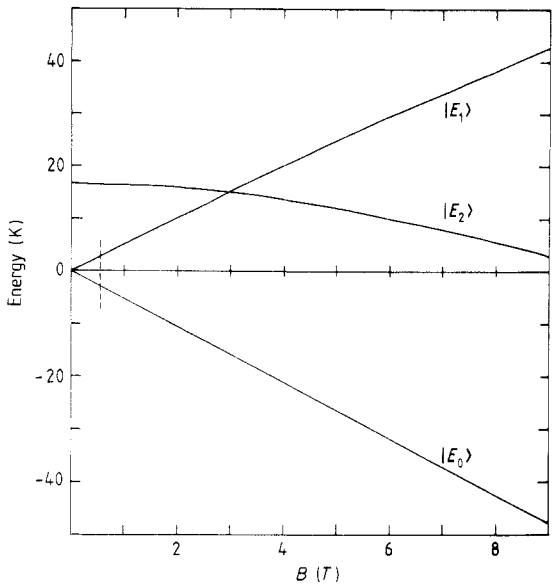

Figure 1. The field dependence of the three lowest energy levels of Ho^{3+} in $Ho(OH)_3$, calculated from the crystal-field parameters of Scott (1970). As in all diagrams except figure 3, the field is along the crystallographic *c* axis. The vertical broken line corresponds to zero applied field at 1.4 K (see equations (4) and (9)).

0 and at $B_a = 8$ T, the highest field applied in this work, in terms of the eigenstates $|M\rangle$ of J_c. All other states are at least 100 K above the ground state. $|E_2\rangle$ has negligible population at the temperatures and fields at which our NMR measurements were made, but makes an important contribution to the measured hyperfine splitting through second-order terms; in addition, it is responsible for most of the transverse susceptibility (table 1) on which the NMR enhancement factor depends. *Qualitatively* similar conclusions follow from the crystal-field parameters of Karmakar and co-workers.

The field dependences of $\langle J_c\rangle$ and of $\langle O_2^0\rangle = \langle 3J_c^2 - J^2\rangle$ for the states $|E_0\rangle$ and $|E_1\rangle$ are shown in figure 2. These expectation values determine the first-order intra-ionic hyperfine splitting of each state (see § 2.4). The finite polarisability of the ground state and hence the longitudinal susceptibility of the material at low temperatures (table 1) is due to the existence of higher states, the lowest of which is at about 150 K, connected to $|E_0\rangle$ by J_c (see also § 4). Also shown in figure 2 is the thermal average

$$\langle J_c\rangle_T = p_0\langle E_0|J_c|E_0\rangle + p_1\langle E_1|J_c|E_1\rangle \tag{8}$$

where p_0 and p_1 are respectively the occupation probabilities of $|E_0\rangle$ and $|E_1\rangle$, calculated at 1.4 K and at 4.2 K.

Table 3. Eigenstates $|E_0\rangle$ $|E_1\rangle$ $|E_2\rangle$ of Ho^{3+} at $B_a = 0$ in the ferromagnetic state (1.4 K) and at $B_a = 8$ T, calculated from the crystal-field parameters of Scott (1970). Basis: eigenfunctions $\{|M\rangle\}$ of J_c.

	$B_a = 0$ ($B = 0.54$ T)	$B_a = 8$ T ($B = 8.49$ T)
$\|E_0\rangle$	$0.940\|7\rangle + 0.308\|1\rangle + 0.144\|-5\rangle$	$0.963\|7\rangle + 0.251\|1\rangle + 0.092\|-5\rangle$
$\|E_1\rangle$	$0.935\|-7\rangle + 0.318\|-1\rangle + 0.155\|5\rangle$	$0.866\|-1\rangle + 0.416\|-1\rangle + 0.278\|5\rangle$
$\|E_2\rangle$	$0.606\|6\rangle + 0.571\|0\rangle + 0.553\|-6\rangle$	$0.798\|6\rangle + 0.501\|0\rangle + 0.334\|-6\rangle$

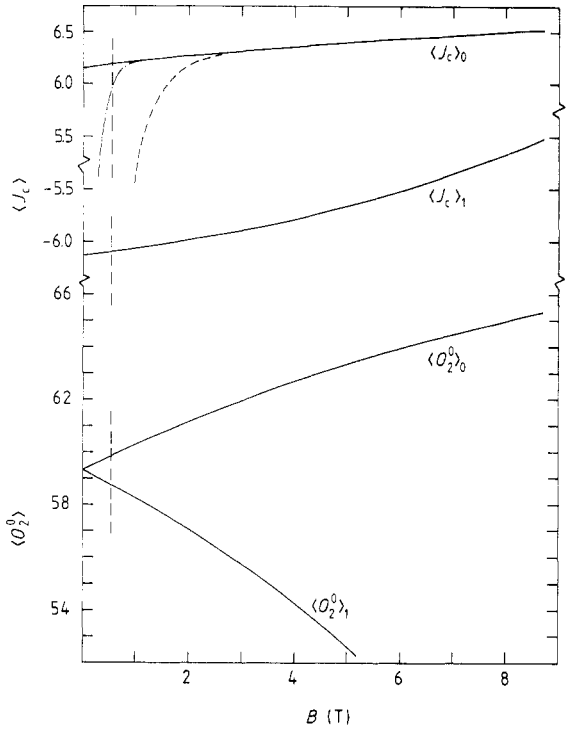

Figure 2. The calculated field dependence of the expectation values of J_c and of O_2^0 for the states $|E_0\rangle$ and $|E_1\rangle$. Also shown are the calculated thermal averages of J_c at 1.4 K and 4.2 K (broken curves). The calculations are based on the crystal-field parameters of Scott (1970). The vertical broken line corresponds to zero applied field (see equations (4) and (9)).

2.3. The molecular field

The molecular field B_m is the sum of the dipolar field B_{dip} and the exchange field B_{ex}, both of which we assume to be proportional to the thermal average $\langle J_c \rangle_T$. The total molecular field B_m may be deduced from Scott's optical measurement of the spontaneous Zeeman splitting of the ground doublet $\{|E_0\rangle, |E_1\rangle\}$. Scott's data give $E_1 - E_0 = (5.6 \pm 0.3)$ K at 1.3 K with $B_a = 0$; the corresponding values of B ($= B_m$: see equation (4)) and of $\langle J_c \rangle_T$ are respectively (0.55 ± 0.03) T and 6.03 ± 0.04 (see figures 1 and 2) and we conclude that

$$B_m = (0.091 \pm 0.004)\langle J_c \rangle_T \text{ T}. \tag{9}$$

A straightforward lattice sum based on the lattice parameters given in table 1 gives

$$B_{dip} = 0.122\langle J_c \rangle_T \text{ T}. \tag{10}$$

This expression includes the Lorentz field and the average demagnetising field within the needle-shaped crystals. Comparison with equation (9) shows that the exchange contribution to the total molecular field is relatively small and negative, in qualitative agreement with the findings of Catanese and Meissner (1973).

Before concluding this section we briefly consider electrostatic multipolar interactions between the holmium ions. The quadrupole–quadrupole term, within the mean-field approximation, is proportional to $\langle O_2^0 \rangle_T O_2^0$ and so may be represented as a contribution to the leading term in the crystal-field interaction (equation (2)). (See also

Table 4. Contributions to the ground-state hyperfine parameters of Ho^{3+} at $B_a = 0$ T in the ferromagnetic state ($T = 1.4$ K) and at $B_a = 8.0$ T, based on the crystal-field parameters of Scott (1970). Units: MHz.

	Dipolar			Quadrupolar			Octupolar
	$a'^{(1)}$	$a'^{(2)}$	a''	$P'^{(1)}$	$P'^{(2)}$	P''	w
$B_a = 0$ ($B = 0.54$ T)	5019.9	7.0	6.5	31.3	11.1	−26.8	0.217
$B_a = 8$ T ($B = 8.59$ T)	5294.0	2.2	78.3	34.1	5.17	−26.1	0.136

Kahle *et al* 1986.) The contribution of the ionic quadrupole moments to the electric field gradients at a given lanthanide site is $V_{cc}^{Q} = -(3/2)(e\langle J\|\alpha_2\|J\rangle\langle r^2\rangle\langle O_2^0\rangle_T/\varepsilon_0)S_q$ where S_q is an appropriate lattice sum (see McCausland and Mackenzie 1979). Numerical evaluation for $Ho(OH)_3$ gives $V_{cc}^{Q} \simeq 6 \times 10^{17}$ V m^{-2}. Setting $\gamma_E \simeq 0.5$ (see Blok and Shirley 1966) in equation (7) we find that the 'quadrupolar' contribution to B_2^0 is ≃4 mK, less than the uncertainty on either of the values of B_2^0 given in table 2. It is unlikely that higher-order multipolar terms will be of any greater importance.

2.4. *The effective nuclear Hamiltonian*

As in I, we describe the hyperfine splitting in terms of an effective nuclear spin Hamiltonian containing dipolar, quadrupolar and octupolar terms:

$$\mathcal{H} = h\{a_t I_z + P_t(I_z^2 - I^2/3) + wI_z^3\} \tag{11}$$

where $\boldsymbol{I}$ is the nuclear spin operator. The z axis is here defined by the direction of $\langle \boldsymbol{J}\rangle_T$ which, in almost all of the present work, is collinear with the crystallographic $\boldsymbol{c}$ axis.

The dipolar parameter is the sum of intra- and extra-ionic terms:

$$a_t = a' + a''. \tag{12}$$

The intra-ionic term a' is dominated by the first-order contribution

$$a'^{(1)} = A\langle J_z\rangle = A\langle J_c\rangle \tag{13}$$

where A is the free-ion dipolar coupling coefficient (Appendix 2). An expression for the relatively small second-order contribution $a'^{(2)}$ is given in Appendix 1. The extra-ionic contribution a'', which is also small compared to $a'^{(1)}$, is proportional to the sum of the dipolar and applied fields; using the nuclear moment given in Appendix 2, we obtain

$$a'' = (8.9 \pm 0.1)B'' \text{ MHz} \tag{14}$$

where $B'' = B_a + B_{dip}$ is in tesla. The relative importance of the various contributions to a_t can be judged from table 4.

The quadrupole parameter is also the sum of intra- and extra-ionic terms:

$$P_t = P' + P''. \tag{15}$$

The first-order contribution to P' may be written in the form

$$P'^{(1)} = C\langle 3J_z^2 - J^2\rangle = C\langle O_2^0\rangle \tag{16}$$

since $O_2^0 = 3J_c^2 - J^2$ and $J_c = J_z$; $C = P_0'/[J(2J-1)]$ is a measure of the free-ion quadrupolar coupling (Appendix 2). An expression for $P'^{(2)}$, the second-order (pseudo-quadrupole) contribution to P', is given in Appendix 1†. P'', the extra-ionic term, is

† Our notation here follows that of McCausland and Mackenzie (1979), not that of Blok and Shirley (1966).

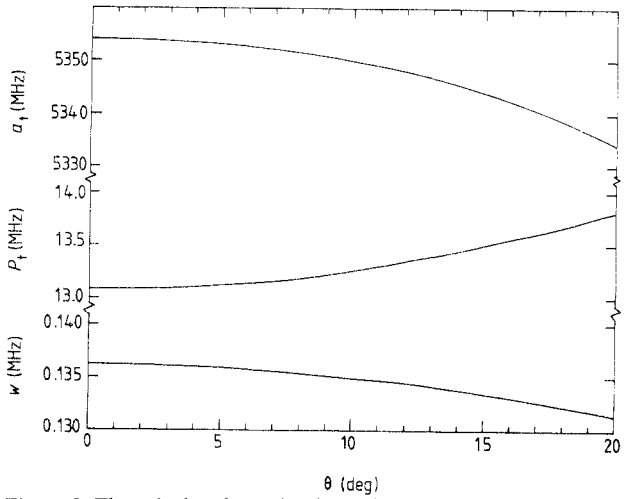

Figure 3. The calculated angular dependence of the hyperfine parameters in a field of 8 T. θ is the angle between the field and the crystallographic c axis. The value assumed for the extra-ionic electric-field gradient is that obtained in I. Crystal-field parameters are taken from Scott (1970).

related to V_{cc}, the extra-ionic electric field gradient, by

$$P'' = 3(e/h)Q_n\gamma_N V_{cc}/4I(2I-1) \tag{17}$$

where I and Q_n are respectively the nuclear spin and quadrupole moment (Appendix 2); γ_N is the nuclear anti-shielding factor in the notation of Edmonds (1963). ($\gamma_N = 1 - \gamma_\infty$ in the notation of Blok and Shirley (1966).) Unlike the dipolar case, all three contributions to P_t are of comparable magnitude: see table 4. Eliminating V_{cc} between equations (7) and (17) and using the data in Appendix 2, we obtain

$$\gamma_N/\gamma_E = (1-\gamma_\infty)/(1-\sigma_2) = (4.07 \pm 0.03)[P''/B_2^0] \tag{18}$$

where P'' is in MHz and B_2^0 is in K.

An expression for the pseudo-octupole parameter w, which arises from a cross term between the free-ion dipolar and quadrupolar interactions, is given in Appendix 1.

The angular dependence of the calculated ground-state hyperfine parameters at 8 T, shown in figure 3, indicates that the hyperfine splitting is insensitive to minor misalignment of the applied field with the c axis. The behaviour of the hyperfine parameters when $\boldsymbol{B}_a$ is collinear with the c axis is shown in figures 5 to 8 below; see also table 4.

Before proceeding further, we need to consider whether the expectation values appearing in equations (13) and (16) pertain to the electronic ground state or to a thermal average (cf equation (8)). The latter situation, in which the hyperfine parameters are averaged by rapid fluctuations of the parent ion, is the one normally encountered in magnetic materials (Winter 1962, Gruner and Tompa 1972, Cha and Cowan 1974, McCausland and Mackenzie 1979). In I, however, we argued that the observed nuclear relaxation rate in ferromagnetic $Ho(OH)_3$ cannot readily be reconciled with the optical linewidth if the hyperfine parameters are thermally averaged. Inspection of the graphs of $\langle J_c \rangle$ in figure 2 shows that the behaviour of the hyperfine splitting in low fields offers an independent test of that argument.

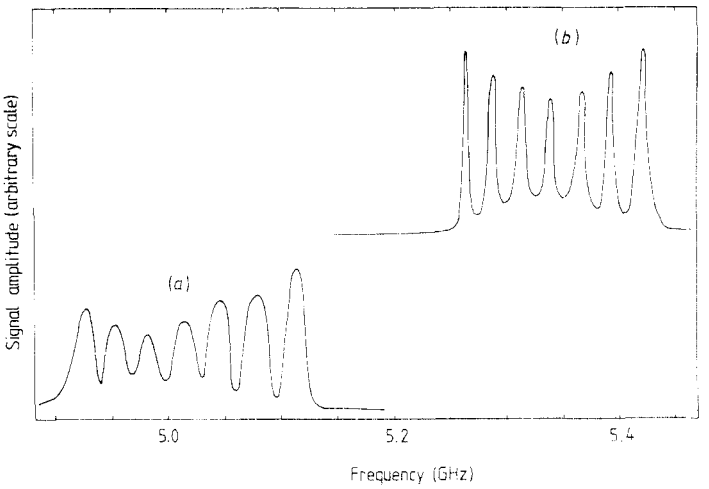

Figure 4. NMR spectra of ^{165}Ho in a single crystal of $Ho(OH)_3$. (*a*) Free-precession spectrum in zero applied field ($T = 1.4$ K); (*b*) spin-echo spectrum with a field of 8 T applied along the *c* axis ($T = 4.2$ K).

3. Experimental details

The crystals of holmium hydroxide used in this work were supplied by Dr S Mroczkowski of Yale University. For each set of measurements a single crystal, approximately 5 mm in length and 0.5 mm in diameter, was mounted on the central conductor of a coaxial resonant cavity tunable from 4 to 6 GHz. The long axis of the crystal, which coincides with the crystallographic *c* axis, was visually aligned with the central conductor which, in turn, is coaxial with the 8 T superconducting solenoid providing the field. The maximum misalignment of the *c* axis with the applied field is estimated to be about 3°. The calculated angular dependence of the hyperfine parameters (figure 3) indicates that a misalignment of that order would have negligible effect on the hyperfine splitting, a conclusion which we have confirmed by NMR measurements on deliberately misaligned specimens.

Our measurements were made by pulsed NMR at liquid-helium temperatures. Good thermal contact between sample and coolant was assured by admitting the liquid helium to the interior of the cavity. Pulse durations were of the order of 50 ns. The calculated NMR enhancement factor (see, for example, McCausland and Mackenzie 1979) falls from about 50 in zero field to about 25 in 8 T, but this is more than compensated by an increase in the transverse relaxation time as the field is increased. Strong spin-echo signals were obtained at 4.2 K in fields above 5 T, but when B_a was reduced to 2.5 T the echoes were barely visible even when the temperature was lowered to 1.4 K and the pulse separation reduced to its minimum usable value of 200 ns. Our low-field spectra were therefore obtained from free-precession signals following 90° pulses.

4. Results and discussion

NMR spectra were taken on several different samples at fields between $B_a = 0$ ($B = 0.54$ T) and $B_a = 8$ T ($B = 8.59$ T). Representative spectra at low and high fields are shown in figure 4. Each spectrum was fitted to the effective spin Hamiltonian (11). In what follows, the measured hyperfine parameters a_t, P_t and w are presented as functions

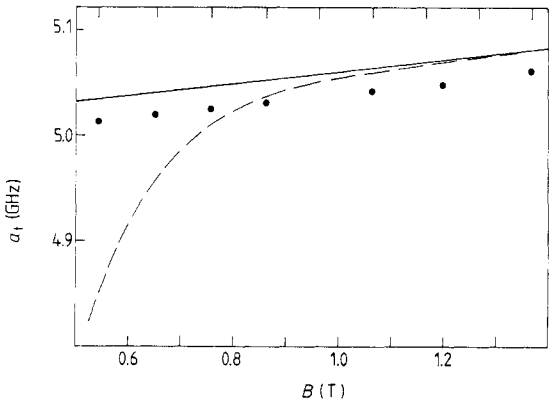

Figure 5. The calculated and measured behaviour of the dipolar hyperfine parameter a_t in low fields. The full line shows the calculated variation of a_t in the ground state $|E_0\rangle$; the broken curve represents the calculated behaviour of a_t at 1.4 K if the hyperfine splitting is thermally averaged. Both curves are based on the crystal-field parameters of Scott (1970). The experimental results (full circles) were taken at 1.4 K; the uncertainty is comparable to the size of the full circles.

of the total field $B = B_a + B_m$.

In figure 5 we compare the low-field behaviour of a_t, the magnetic dipole hyperfine parameter measured at 1.4 K, with the calculated curves for the electronic ground state and for a thermal average over $|E_0\rangle$ and $|E_1\rangle$. The almost linear field dependence of the measured parameter is totally at variance with the thermal averaging model, and confirms that the observed hyperfine splitting is a property of the ground state alone. (The small and almost constant discrepancy between the solid curve and the experimental points is discussed in § 5.) The same *qualitative* conclusion is obtained with the crystal-field parameters of Karmakar *et al* (1981a, b), albeit with a much larger offset between calculated and measured hyperfine parameters (see figure 6). The result just obtained

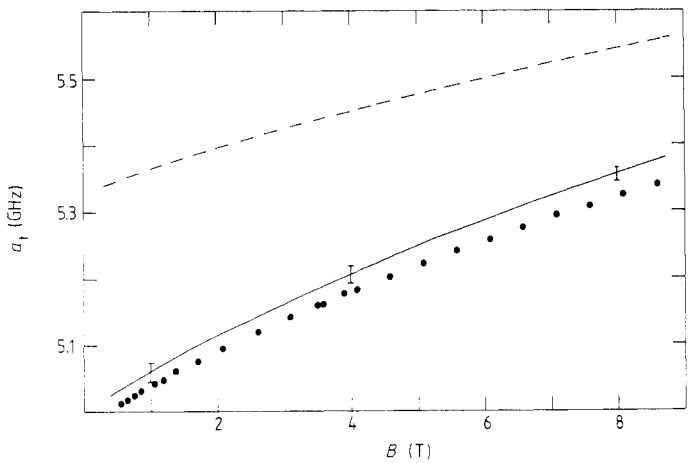

Figure 6. The behaviour of the dipolar hyperfine splitting in applied fields up to 8 T. The uncertainty on the experimental results (full circles) is smaller than the size of the full circle. The full and broken curves represent theoretical calculations based on the crystal-field parameters of Scott (1970) and Karmakar *et al* (1981a, b) respectively.

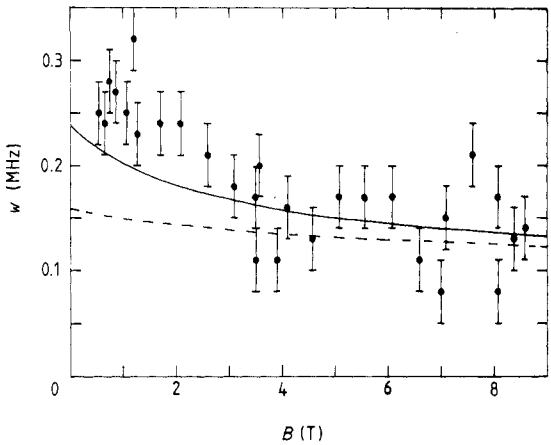

Figure 7. The behaviour of the octupolar hyperfine parameter in applied fields up to 8 T. The full and broken curves represent theoretical calculations based on the crystal-field parameters of Scott (1970) and Karmakar *et al* (1981a, b) respectively.

implies that the τ_0, the lifetime of the ionic ground state, cannot be less than the nuclear transverse relaxation time. From our observations of the nuclear relaxation rate we conclude that $\tau_0 > 200$ ns when $T = 1.4$ K and $B_a = 0$, whereas $\tau_0 > 2\,\mu$s when $T = 4.2$ K and $B = 8$ T.

In the remainder of this paper, all calculated hyperfine parameters pertain to the ground state $|E_0\rangle$. In figure 6 we compare the measured field dependence of a_t over the entire experimental range of fields with theoretical calculations based on the crystal-field parameters of Scott (1970) and Karmakar *et al* (1981a, b). The error bars on the full curve are derived from the error matrix given by Scott and from the quoted uncertainties on all other constants entering the calculation: see Appendix 2 for details. We have not been able to assign error bars to the broken curve because the off-diagonal elements of the error matrix for the crystal-field parameters of Karmakar and co-workers are unknown. The diagonal elements, however, are comparable to those of Scott (see table 2), so the error bars for the two curves are probably of the same order of magnitude. We remark in passing that the rate of increase of a_t with the field is some six times greater than that expected from the direct interaction of the nuclear moment with the applied field. This is due to the finite polarisability of the ionic ground state, an effect undetected by conventional magnetisation measurements (see table 1 and equations (20)–(23)).

Although Scott's parameters are based on optical data on the dilute $Ho:Y(OH)_3$ system, it is clear from figure 6 that they give a much more accurate description of the field dependence of the dipolar splitting in $Ho(OH)_3$ than do those of Karmakar and co-workers, which are based on thermal and magnetic measurements on the pure material. A similar conclusion may be drawn from the behaviour of the octupolar parameter (figure 7), but here the experimental scatter is much larger than the uncertainties (not shown) on the calculated values of w. The mean deviations of the measured points from the calculated curves are (18 ± 8) kHz in the case of Scott's parameters and (49 ± 10) kHz in the case of those of Karmakar and co-workers.

In figure 8 we show the calculated field dependence of the intra-ionic contributions to the quadrupole parameter together with our measured values of $|P_t|$. A straightforward comparison between theory and experiment is not possible (i) because the sign of P_t cannot be directly determined from the NMR spectrum (Abragam 1961) and (ii) because

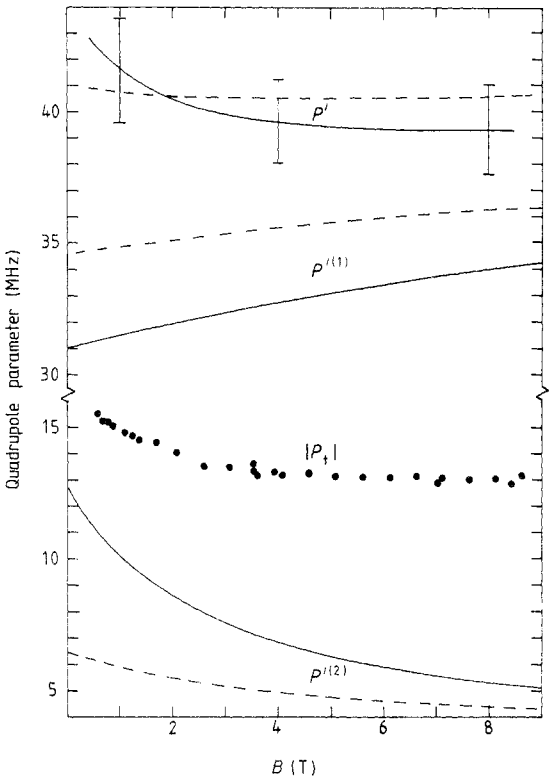

Figure 8. The calculated field dependence of the intra-ionic quadrupolar hyperfine parameter P'. Also shown are the first- and second-order contributions $P'^{(1)}$ and $P'^{(2)}$. The full and broken curves are based on the crystal-field parameters of Scott (1970) and Karmakar *et al* (1981a, b) respectively. The full circles denote the measured values of P_t.

P'', the extra-ionic contribution to P_t, has not yet been calculated *a priori*. We know, however, that V_{cc}, hence $P'' = P_t - P'$ (equation (17)), is independent of the field. Given an accurate set of crystal-field parameters, therefore, we may expect the graph of $|P_t| - P'$ against B to be horizontal if $P_t > 0$; conversely, the graph of $-|P_t| - P'$ against B should be horizontal if $P_t < 0$. It is clear from figure 9 that P_t can be negative only if the crystal-field parameters are grossly in error. As noted in I, the assumption of a positive P_t also gives much better agreement with the electric-field gradient obtained from Mössbauer measurements on ^{155}Gd in $Gd(OH)_3$ (Katila *et al* 1972). We may safely assume that P_t is in fact positive.

Having established the sign of P_t, we may treat the constancy of $P_t - P'$ as a criterion for the accuracy of the crystal-field parameters. Neither of the two curves in the upper part of figure 9 is horizontal, but the one based on Scott's parameters is more nearly so than the one based on the parameters of Karmakar and co-workers. Using Scott's parameters, we find that the mean value of $P'' = P_t - P'$ is (-26.4 ± 2.5) MHz. Substitution of Scott's value of B_2^0 into equation (18) then gives

$$\gamma_N/\gamma_E = 149 \pm 15 \tag{19}$$

for the ratio of antishielding factors, a result in close agreement with that obtained in I. As in I, the uncertainty is dominated by the quadrupolar coupling constant C.

Anti-shielding factors are of course essentially phenomenological devices which

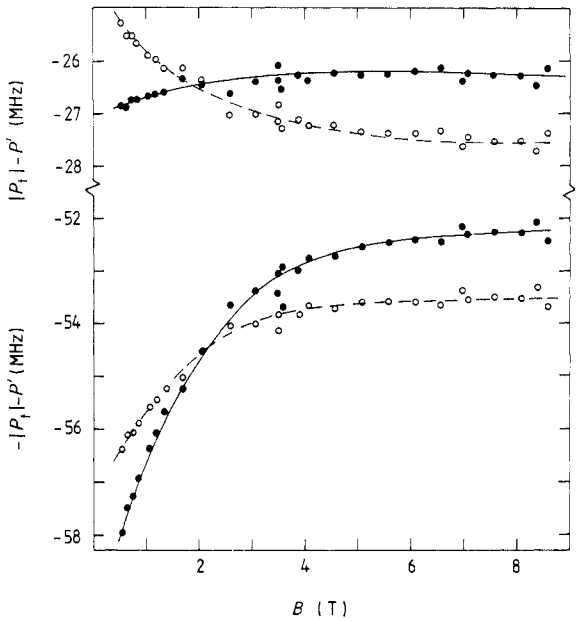

Figure 9. The field dependences of $\pm|P_t| - P'$ derived from the data shown in figure 8. Full circles: based on the crystal-field parameters of Scott (1970). Open circles: based on the crystal-field parameters of Karmakar *et al* (1981a, b). The full and broken curves, corresponding respectively to the full and open circles, are simply to guide the eye.

purport to describe the electric-field gradient arising from closed shells in terms of distortions caused by the extra-ionic electric-field gradient. Now that accurate *ab initio* calculations of V''_{cc}, the total electric-field gradient at the nuclear site, are becoming available (see, for example, Blaha *et al* 1988), it may be useful to note that the value of V''_{cc} $(=\gamma_N V_{cc})$ derived from our measurements is $-(8.7 \pm 0.8) \times 10^{21}\,\mathrm{V\,m^{-2}}$.

One outcome of our work that is practically independent of the accuracy of the crystal-field parameters is a precise determination of the spontaneous magnetisation and the initial longitudinal susceptibility of $Ho(OH)_3$ at $T = 0$. Subtracting the small second-order and extra-ionic terms from a_t and correcting the molecular field for the finite occupation probability (<2%) of $|E_1\rangle$ at 1.4 K (see table 4 and equations (8) and (9)), we obtain

$$a'^{(1)} = [5000.2 \pm 1.4 + (49.3 \pm 1.5)B_a]\,\mathrm{MHz} \tag{20}$$

where B_a is in tesla. (The fit has been restricted to fields below 1 T to avoid non-linear effects.) It follows from equation (13) that the ionic moment at $T = 0$ is

$$\langle\mu\rangle = g\langle J_z\rangle = [7.647 \pm 0.002 + (0.075 \pm 0.002)B_a]\mu_B. \tag{21}$$

Using the lattice parameters given in table 1, we obtain

$$M = [1.181 \pm 0.001 + (0.0116 \pm 0.0004)B_a]\,\mathrm{MA\,m^{-1}} \tag{22}$$

for the initial field dependence of the magnetisation at $T = 0$. The spontaneous magnetisation at $T = 0$ is therefore $M_0 = 1.181 \pm 0.001\,\mathrm{MA\,m^{-1}}$, while the initial axial susceptibility is

$$\chi_\parallel = \mathrm{d}M/\mathrm{d}H = \mu_0\,\mathrm{d}M/\mathrm{d}B_a = 0.0146 \pm 0.0005. \tag{23}$$

(The value of H within the needle-like crystals may, with negligible error, be identified

with B_a/μ_0.) Our values for M_0 and $\chi_{\parallel}$ are compatible with the figures for M_{sat} and $\chi_{\parallel}$ quoted in table 1. Note, however, the superior precision of the NMR results over those obtained from traditional magnetisation measurements.

5. Conclusions

The field dependence of the hyperfine splitting clearly confirms the conclusion that the measured hyperfine parameters pertain solely to the ionic ground state $|E_0\rangle$ (I). It follows that there exists, in principle, a distinct hyperfine spectrum for the excited state $|E_1\rangle$. A search for this spectrum at fields and temperatures such that $|E_1\rangle$ has an appreciable population (>1%) was unsuccessful. The corresponding spectrum has been observed in a dilute (1%) solution of holmium in $Y(OH)_3$ (Carboni 1987; see also Carboni *et al* (1988) for the closely related case of Ho^{3+} in yttrium ethylsulphate). Our failure to detect it in pure $Ho(OH)_3$ is attributed to the much faster relaxation rate in the concentrated material.

We have shown that the crystal-field parameters of Scott (1970) for $Ho:Y(OH)_3$ provide a much better description of the field dependence of the hyperfine splitting in the pure holmium compound than do those of Karmakar *et al* (1981a, b) for $Ho(OH)_3$. This may be due in part to the fact that Scott's parameters were derived from data taken at 77 K, where the effects of thermal expansion are small, whereas those of Karmakar and co-workers are based on measurements in a temperature range (80–300 K) where there is significant variation in the lattice parameters. At any rate, we must conclude that the crystal-field parameters for the dilute and concentrated materials are much more nearly equal than Karmakar and co-workers have supposed.

The residual discrepancy between the measured field dependence of the hyperfine parameters and the predictions of Scott's crystal-field parameters is small but statistically significant, at least in the case of a_t and w (figures 6 and 7). One possible explanation is a slight shift in the crystal-field parameters between 77 K and liquid-helium temperatures; another is that the parameters for Ho^{3+} in $Ho(OH)_3$ differ slightly from those in $Y(OH)_3$. Our NMR measurements in $Ho:Y(OH)_3$ (Bunbury *et al* 1966) do in fact suggest a small difference in the crystal-field parameters but, paradoxically, the difference is such that Scott's parameters describe the hyperfine splitting slightly *less* accurately in the dilute than in the concentrated material! Yet another possible explanation is a host dependence of $\langle r^{-3}\rangle$ for the 4f electrons and hence of the coupling constants A and C. (See, for example, Bleaney 1972). Finally, we recall that we have neglected J-mixing in our analysis. Its effects, though believed to be small in $Ho(OH)_3$, are difficult to quantify and it is just possible that it may make a significant contribution to the observed discrepancy. Careful analysis of hyperfine splittings and optical spectra in different host materials will be required to determine which of the explanations tentatively suggested here is the most important.

Our measurements of the dipolar hyperfine splitting have allowed us to determine the spontaneous magnetisation and the longitudinal susceptibility of holmium hydroxide with a precision considerably greater than that obtained by traditional magnetisation measurements. The quadrupolar splitting, in conjunction with crystal-field parameters derived from optical spectroscopy, confirms our earlier determination of the ratio of nuclear to electronic anti-shielding factors for Ho^{3+} in the hydroxide (I). As noted by Carboni *et al* (1988), the accuracy with which the anti-shielding ratio can now be measured makes it possible, for the first time, to make a reliable assessment of its dependence on the host medium.

Acknowledgments

We are indebted to Professor W P Wolf for bringing the rare-earth hydroxides to our notice and to Dr S Mroczkowski for supplying the specimens. The crystals were grown at Yale with support from NSF Grant DMR-8216222. The financial support of SERC is gratefully acknowledged.

Appendix 1. The hyperfine splitting of the electronic energy levels

The analysis given here is based on that given by McCausland and Mackenzie (1979) and developed by Waind *et al* (1983), with notational changes and adaptations appropriate for the present work.

The hyperfine splitting in the solid may, in normal circumstances, be calculated by treating $\mathcal{H}_{\rm hf}$, the free-ion hyperfine interaction, as a perturbation on the electronic Hamiltonian $\mathcal{H}_{\rm el}$ (equation (1)). It is also necessary to allow for the interaction of the nucleus with extra-ionic fields; it can be shown that the appropriate procedure is to include $\mathcal{H}''$, the extra-ionic interaction, at the first-order stage of the intra-ionic perturbation expansion. For most purposes, including the present work, it is sufficient to carry the perturbation calculation to second order.

The free-ion hyperfine interaction is the sum of the dipolar and quadrupolar terms, $\mathcal{H}_{\rm hfd}$ and $\mathcal{H}_{\rm hfq}$:

$$\mathcal{H}_{\rm hf} = \mathcal{H}_{\rm hfd} + \mathcal{H}_{\rm hfq} \tag{A1.1}$$

where

$$\mathcal{H}_{\rm hfd} = hA\boldsymbol{J}\cdot\boldsymbol{I} \tag{A1.2}$$

and

$$\mathcal{H}_{\rm hfq} = hC[2(\boldsymbol{J}\cdot\boldsymbol{I})^2 + \boldsymbol{J}\cdot\boldsymbol{I} - (2/3)J^2I^2] \tag{A1.3}$$

where $C = P_0'/[J(2J-1)]$ is a measure of the free-ion quadrupolar coupling (see Appendix 2). Equation (A1.3) may be recast in the form

$$\begin{aligned}\mathcal{H}_{\rm hfq} = hC[&(3J_z^2 - J^2)(I_z^2 - I^2/3) + (1/2)(J_+^2I_+^2 + J_-^2I_-^2)\\ &+ (1/2)(J_zJ_+ + J_+J_z)(I_zI_- + I_-I_z)\\ &+ (1/2)(J_zJ_- + J_-J_z)(I_zI_+ + I_+I_z)]\end{aligned} \tag{A1.4}$$

where $J_\pm = J_x \pm iJ_y$; $\{x, y, z\}$ is an arbitrary set of Cartesian coordinates.

It follows from (A1.2) and (A1.4) that the free-ion hyperfine interaction may be expressed as a sum of products of electronic and nuclear operators, $\mathscr{E}_r$ and $\mathscr{N}_r$ respectively:

$$\mathcal{H}_{\rm hf}(\boldsymbol{J}\cdot\boldsymbol{I}) = \sum_r \mathscr{E}_r(\boldsymbol{J})\mathscr{N}_r(\boldsymbol{I}). \tag{A1.5}$$

The intra-ionic hyperfine splitting of a given electronic state $|E_{\rm N}\rangle$ may now be described, to first order in $\mathcal{H}_{\rm hf}/\mathcal{H}_{\rm el}$, by the effective nuclear Hamiltonian

$$\mathcal{H}_N'^{(1)}(\boldsymbol{I}) = \sum_r \langle\mathscr{E}_r\rangle_N\mathscr{N}_r(\boldsymbol{I}) \tag{A1.6}$$

where $\langle - \rangle_N = \langle E_N|--|E_N\rangle$. To this we must add the extra-ionic interaction $\mathcal{H}'' = \mathcal{H}_{\rm d}'' + \mathcal{H}_{\rm q}''$ (see McCausland and Mackenzie (1979) for details), so the total first-order

hyperfine splitting is given by the eigenvalues of

$$\mathcal{H}_N^{(1)} = \mathcal{H}_N'^{(1)} + \mathcal{H}''. \tag{A1.7}$$

The dominant contribution to (A1.7) is the intra-ionic dipolar term $hA\langle \boldsymbol{J}\rangle_N \cdot \boldsymbol{I}$. It is therefore convenient to define the z axis to be parallel to $\langle \boldsymbol{J}\rangle_N$. In general, the z axis thus defined is distinct from the crystallographic $\boldsymbol{c}$ axis, but the two axes coincide in the present work. This special circumstance ensures that all terms in $\mathcal{H}_N^{(1)}$ that do not commute with $I_z(=I_c)$ vanish identically, so (A1.7) assumes the simple form

$$\mathcal{H}_N^{(1)} = h[(a_N'^{(1)} + a'')I_z + (P_N'^{(1)} + P'')(I_z^2 - I^2/3)] \tag{A1.8}$$

where

$$a_N'^{(1)} = A\langle J_z\rangle_N \tag{A1.9}$$

and

$$P_N'^{(1)} = C\langle 3J_z^2 - J^2\rangle_N = C\langle O_2^0\rangle_N \tag{A1.10}$$

are the first-order intra-ionic dipolar and quadrupolar hyperfine parameters, respectively. The extra-ionic parameters a'' and P'' are related to the extra-ionic magnetic field and to the extra-ionic electric field gradient by equations (14) and (17) respectively.

The second-order corrections to the hyperfine levels ε_{Nn} derived from (A1.7) are given by

$$\delta\varepsilon_{Nn} = \langle \varepsilon_{Nn}|\mathcal{H}_N'^{(2)}|\varepsilon_{Nn}\rangle \tag{A1.11}$$

where $|\varepsilon_{Nn}\rangle$ is the eigenstate of (A1.7) belonging to ε_{Nn} and

$$\mathcal{H}_N'^{(2)} \sum_{r,s} \sum_{M\neq N} \frac{\langle E_N|\mathcal{C}_r|E_M\rangle\langle E_M|\mathcal{C}_s^\dagger|E_N\rangle\mathcal{N}_r\mathcal{N}_s^\dagger}{E_N - E_M} \tag{A1.12}$$

where $\dagger$ denotes the Hermitian conjugate. In the present case ($z \parallel \boldsymbol{c}$) the eigenstates $|E_{Nn}\rangle$ of $\mathcal{H}_N^{(1)}$ coincide with the eigenstates $|m\rangle$ of I_z ($-I < m < I$) and $\mathcal{H}_N'^{(2)}$ assumes the simple form

$$\mathcal{H}_N'^{(2)} = h[a_N'^{(2)}I_z + P_N'^{(2)}I_z^2 + w_N I_z^3]. \tag{A1.13}$$

The dominant contributions to the pseudo-dipole and pseudo-quadrupole terms, $a_N'^{(2)}$ and $P_N'^{(2)}$ respectively, are of order $hA^2/\Delta E$, where ΔE is a representative electronic energy denominator; the pseudo-octupole term w_N, of order $hAC/\Delta E$, is at least an order of magnitude smaller. Terms of order $hC^2/\Delta E$ are insignificant and have been omitted. Explicit expressions for the coefficients in (A1.13) are given below.

$$a_N'^{(2)} = (A^2/4)(S_{2N} - S_{3N}) + AC\{[I(I+1) - 1/2](S_{5N} + S_{6N}) - 2I(I+1)S_{4N}\} \tag{A1.14}$$

$$P_N'^{(2)} = (A^2/4)(4S_{1N} - S_{2N} - S_{3N}) + (3/2)AC(S_{5N} - S_{6N}) \tag{A1.15}$$

$$w_N = AC(6S_{4N} - S_{5N} - S_{6N}). \tag{A1.16}$$

Here the S_{qN} ($q = 1$ to 6) denote sums over the electronic eigenstates:

$$S_{qN} = h \sum_{M\neq N} \frac{T_{qNM}}{E_N - E_M} \tag{A1.17}$$

where

$$\begin{aligned}
T_{1NM} &= |\langle E_N|J_z|E_M\rangle|^2 \\
T_{2NM} &= |\langle E_N|J_-|E_M\rangle|^2 \\
T_{3NM} &= |\langle E_N|J_+|E_M\rangle|^2 \\
T_{4NM} &= \mathrm{Re}\{\langle E_N|J_z^2|E_M\rangle\langle E_M|J_z|E_N\rangle\} \\
T_{5NM} &= \mathrm{Re}\{\langle E_N|J_+|E_M\rangle\langle E_M|J_-J_z + J_zJ_-|E_N\rangle\} \\
T_{6NM} &= \mathrm{Re}\{\langle E_N|J_-|E_M\rangle\langle E_M|J_+J_z + J_zJ_+|E_N\rangle\}.
\end{aligned} \tag{A1.18}$$

Our definitions of the S_{jN} differ from those given by Waind *et al* (1983) by certain numerical factors that have been transferred to equations (A1.14)–(A1.16). A misprint in (A.1) of Waind *et al* (1983) has also been corrected.

The total hyperfine splitting of the electronic eigenstate $|E_N\rangle$ is now given by the effective Hamiltonian

$$\mathcal{H}_N = h[a_{tN}I_z + P_{tN}(I_z^2 - I^2/3) + w_N I_z^3] \tag{A1.19}$$

where

$$a_{tN} = a'_N + a'' = a'^{(1)}_N + a'^{(2)}_N + a'' \tag{A1.20}$$

and

$$P_{tN} = P'_N + P'' = P'^{(1)}_N + P'^{(2)}_N + P''. \tag{A1.21}$$

If electronic relaxation is sufficiently rapid then, as noted in I, the observed hyperfine splitting will be a thermal average over states $|E_N\rangle$ with significant populations, namely $|E_0\rangle$ and $|E_1\rangle$ in the case under discussion; individual hyperfine splittings for each state are observed only in the limit of slow electronic relaxation. In order not to prejudice the discussion of this point the subscript N is omitted in § 2.4.

Appendix 2. Numerical constants and error analysis

The statistical uncertainty on the calculated hyperfine splitting is derived from quoted uncertainties on the crystal-field parameters, on the hyperfine parameters and, where appropriate, on the nuclear moments. Thus, for example, the mean-square uncertainty on the calculated value of a_t is given by

$$\langle(\delta a_t)^2\rangle = \sum_{r,s} \frac{\partial a_t}{\partial \eta_r}\frac{\partial a_t}{\partial \eta_s}\langle \delta\eta_r \delta\eta_s\rangle \tag{A2.1}$$

where the η_r formally denote the quantities B_n^m, A and μ_N. Only in the case of the crystal-field parameters do we expect non-vanishing correlation terms, i.e. terms with $r \neq s$. The complete error matrix for the crystal-field parameters of Scott (1970) is given below. Units: K^2

$$[\langle \delta B_n^m \delta B_{n'}^{m'}\rangle] = \begin{array}{c} \\ B_2^0 \\ B_4^0 \\ B_6^0 \\ B_6^6 \end{array} \begin{array}{c} \begin{array}{cccc} B_2^0 & B_4^0 & B_6^0 & B_6^6 \end{array} \\ \begin{bmatrix} 9.7\times10^{-5} & -7.9\times10^{-8} & 8.6\times10^{-10} & -6.5\times10^{-9} \\ -7.9\times10^{-8} & 2.7\times10^{-9} & -6.9\times10^{-12} & 1.5\times10^{-11} \\ 8.6\times10^{-10} & -6.9\times10^{-12} & 3.3\times10^{-13} & 9.0\times10^{-14} \\ -6.5\times10^{-9} & 1.5\times10^{-11} & 9.0\times10^{-14} & 3.1\times10^{-11} \end{bmatrix} \end{array} \tag{A2.2}$$

Other quantities used in our calculations are as follows.

Properties of Ho^{3+} in the nominally $^5I_8$ ground manifold. Mean-square radius of 4f shell: $\langle r^2\rangle = 2.085 \times 10^{-21}$ m^2 (Freeman and Desclaux 1979); Landé g-factor: 1.242 (Rajnak and Krupke 1967). Operator-equivalent coefficients: see table 2.

Properties of ^{165}Ho. Abundance: 100%; spin $I = 7/2$; magnetic dipole moment $\mu_N = (4.09 \pm 0.05)$ nuclear magneton (Haberstroh *et al* 1972); electric quadrupole moment $Q_N = (3.51 \pm 0.02) \times 10^{-28}$ m^2 (see I).

Hyperfine coupling parameters for $^{165}Ho:Ho^{3+}$. Dipolar: $A = a_0'/J = (812.1 \pm 1.0)$ MHz; quadrupolar: $C = P_0'/[J(2J-1)] = (0.523 \pm 0.026)$ MHz (Bleaney 1972).

The relative contributions of the crystal-field parameters (CFP), the hyperfine coupling parameters (HFP) and the nuclear moment (NM) to the mean-square uncertainties on calculated hyperfine parameters are set out below. Units: MHz^2.

	$\langle(\delta a_t)^2\rangle$			$\langle(\delta P')^2\rangle$		$\langle(\delta w)^2\rangle$	
B_a (T)	CFP	HFP	NM	CFP	HFP	CFP	HFP
0	309	38	0.006	0.3	2.5	0.0002	0.0001
8	77	43	0.9	0.3	2.9	$<10^{-5}$	0.00005

Note that whereas the uncertainty on the calculated dipolar splittings arises mainly from the crystal-field parameters, the uncertainty on the calculated quadrupolar splitting is dominated by the coupling constant C.

References

Abragam A 1961 *The Principles of Nuclear Magnetism* (Oxford: OUP).

Abragam A and Bleaney B 1971 *Résonance Paramagnétique Electronique des Ions de Transition* (Paris: Presses Universitaires de France).

Blaha P, Schwarz K and Dederichs P H 1988 *Phys. Rev.* B **37** 2792–5

Bleaney B 1972 *Magnetic Properties of Rare Earth Metals* ed. R J Elliott (London: Plenum) pp 383–420

Blok J and Shirley D A 1966 *Phys. Rev.* **143** 278–83

Bunbury D St P, Carboni C and McCausland M A H 1985 *J. Phys. C: Solid State Phys.* **18** L1151–5

—— 1986 *Proc. 23rd Congress Ampère (Rome) 1986* (Rome: Istituto Superiore di Sanità) pp 442–3

Carboni C 1987 *PhD Thesis* University of Manchester

Carboni C, Cone R L, Han Z-P and McCausland 1988 *Proc. ICM88; J. Physique* at press

Catanese C A and Meissner H E 1973 *Phys. Rev.* B **8** 2060–74

Catanese C A, Skjeltorp A T, Meissner H E and Wolf W P 1973 *Phys. Rev.* B **8** 4223–46

Cha C L and Cowan D L 1974 *Bull. Am. Phys. Soc.* **19** 202

Chirico R D, Boerio-Goates J and Westrum E F 1981 *J. Chem. Thermodyn.* **13** 1087–94

Christensen A N, Hazell R G and Nielson A 1967 *Acta Chem. Scand.* **21** 481–92

Cochrane R W, Wu C Y and Wolf W P 1971 *J. Appl. Phys.* **42** 1568–9

Cone R L 1972 *J. Chem. Phys.* **57** 4898–903

Cone R L and Faulhaber R 1971 *J. Chem. Phys.* **55** 5198–206

Cone R L and Wolf W P 1978 *Phys. Rev.* B **17** 4162–80

Edmonds D T 1963 *Phys. Rev. Lett.* **10** 129–31

Freeman A J and Desclaux J P 1979 *J. Magn. Magn. Mater.* **12** 11–21

Gruner G and Tompa K 1972 *J. Phys. F: Met. Phys.* **3** 189–98

Haberstroh R A, Moran T I and Penselin 1972 *Z. Phys.* **252** 421–7

Kahle H G, Kasten A, Scott P D and Wolf W P 1986 *J. Phys. C: Solid State Phys.* **19** 4153–68

Karmaker S, Saha M and Ghosh D 1981a *Indian J. Phys.* A **55** 254–8

—— 1981b *J. Appl. Phys.* **52** 4156–61

Katila T E, Typpi V K and Shenoy G K 1972 *Solid State Commun.* **11** 1147–50

McCausland M A H and Mackenzie I S 1979 *Adv. Phys.* **28** 305–456

Morrison C A and Leavitt R P 1982 *Handbook of the Physics and Chemistry of the Rare Earths* vol 5, ed. K A Gschneider and L Eyring (Amsterdam: North-Holland) pp 461–692

Mroczkowski S, Eckert J, Meissner H and Doran J C 1970 *J. Cryst. Growth* **7** 333–42

Prakash O, Bunbury D St P and McCausland M A H 1984 *Z. Phys.* B **58** 39–48

Rajnak K and Krupke W F 1967, *J. Chem. Phys.* **46** 3532–42

Schlachetzki A and Eckert J 1972 *Phys. Status Solidi* a **11** 611–22

Scott P D 1970 *PhD Thesis* Yale University
Scott P D, Meissner H E and Crosswhite H M 1969 *Phys. Lett.* **28A** 489–90
Skjeltorp A T, Catanese C A, Meissner H E and Wolf W P 1973 *Phys. Rev.* B **7** 2062–91
Waind P R, Mackenzie I S and McCausland M A H 1983 *J. Phys. F: Met. Phys.* **13** 1041–56
Winter J M 1962 *J. Physique Radium* **23** 556–64
Wolf W P, Meissner H E and Catanese C A 1968 *J. Appl. Phys.* **39** 1134–6
Wybourne B G 1962 *J. Chem. Phys.* **37** 1807–11